α-Gallium(010) surface reconstruction: A LEED structural analysis of the (1×1) room temperature and $(2\sqrt{2} \times \sqrt{2})\mathbf{R}45^\circ$ low temperature structures

S. Moré*

Institute for Molecular Science, Myodaiji, Okazaki, Aichi 444-8585, Japan

E.A. Soares[1,2,**] and M.A. Van Hove[1,3,4]

[1]*Materials Sciences Division, Lawrence Berkeley National Laboratory, Berkeley, CA 94720, USA,* [2] *Instituto de Fisica Gleb Wataghin, UNICAMP, CP 6165, Campinas, SP, Brazil, 13083-970,* [3]*Advanced Light Source, Lawrence Berkeley National Laboratory, Berkeley, CA 94720, USA,* [4]*Department of Physics, University of California-Davis, Davis, CA 95616, USA.*

S. Lizzit

Sincrotrone Trieste, S.S. 14 Km. 163.5, 34012 Trieste, Italy

A. Baraldi

Dipartimento di Fisica, Universitá di Trieste, Via Valerio 2, 34127 Trieste, Italy and Laboratorio TASC-INFM, S.S. 14 Km. 163.5, 34012 Trieste, Italy.

Ch. Grütter and J.H. Bilgram

Laboratorium für Festkörperphysik, Eidgenössische Technische Hochschule, 8093 Zürich, Switzerland

Ph. Hofmann*

Institute for Storage Ring facilities, University of Aarhus, DK-8000 Aarhus C, Denmark

Abstract

The geometric structure of the *alpha*-Ga(010)-(1×1) room temperature structure and its ($2\sqrt{2}\times\sqrt{2}$)R45° reconstruction below 232 K have been determined using Low Energy Electron Diffraction (LEED) structure analysis. The room temperature structure conforms to the cut-dimer model, forming a two-dimensional metallic structure with only minimal lateral displacements of the atoms. The topmost interlayer distance is 1.53 Å, corresponding to a spacing expansion of 2% from the bulk. In the low-temperature structure, the surface atoms shift to dimerize within the top two layers, resulting in a network of mostly covalent bonds, which form both parallel and perpendicular to the surface plane. The bond lengths of some of these dimers are about 10% shorter than the bond length found in the α-Ga bulk

and are thus shorter than any Ga-Ga bonds reported so far.

PACS numbers: 68.35.Bs

Keywords:

I. INTRODUCTION

α-Gallium is the stable phase of the gallium at atmospheric pressure and the one that forms below the solid-liquid phase transition[1,2]. Its bulk structure is face-centered orthorhombic with eight atoms per unit cell. Each atom has only one nearest neighbor at a distance of 2.44 Å so that the structure can be viewed as being composed of covalent Ga_2 dimers or molecules. Metallicity is only present in the so-called buckled planes, where the ends of the dimers overlap, leading to a strong anisotropy in the Fermi surface and the transport properties. In fact, it is appropriate to view α-Gallium as a solid in which molecular and metallic properties are present simultaneously[3]. Another unusual property of α-Ga is its low melting temperature of only 303 K which means that it should be an ideal candidate for the experimental investigation of surface melting. For the (010) face[4], however, optical[5] and Scanning Tunneling Microscopy (STM)[6] measurements indicate a strong resistance against surface melting. Indeed, the surface melting temperature appears to be *higher* than its bulk counterpart[6]. The properties of this surface have been further investigated with X-ray Diffraction[7], Angle Resolved Photoemission (ARUPS)[8,9], Spot Profile Analysis (SPA) LEED[10] and first-principles calculations[11].

Investigations of the α-Ga(010) surface have revealed a reversible phase transition from the (1×1) room temperature (RT) cell to a $(2\sqrt{2}\times\sqrt{2})$R45° reconstruction at 232 K[8,9]. Later an additional splitting of the $(\pm 1/2, \pm 1/2)$ spot was found with SPA-LEED[10]. It corresponds to a real-space periodicity of about 18 times the size of the unit cell. This splitting is too small to be observed in a standard LEED setup. Recent ARUPS investigations have suggested that the phase transition is accompanied by a sharp decrease of the density of states at the Fermi level and favored by the presence of strong electron-phonon coupling[9].

The delicate balance between being a metal and a molecular solid should be severely disturbed at the surfaces of α-Ga where the co-ordination of the atoms is changed and the symmetry is broken. Pronounced differences in surface and bulk electronic properties have been found for other semi-metals, i.e. for materials where covalent and metallic bonding coexist and the density of bulk states at the Fermi level is low. Examples are the surfaces of Be[12,13] and Bi[14–16] which are much more metallic than the bulk. In the case of α-Ga(010) the situation is more involved because of the phase transition. It appears that the high-temperature structure is more metallic than the low temperature structure and, indeed, such

temperature-dependent metal-insulator transitions may be expected for cases like this[17]. However, the determination of the actual surface geometry is a necessary precondition for an in-depth understanding of the driving forces which trigger the phase transition.

The α-Ga elementary cell is depicted in Fig. 1. The [010]-direction is almost parallel to the direction of the dimers in the bulk. Two distinct terminations of an unreconstructed α-Ga surface are possible. The so-called A termination is a configuration where the dimer bonds remain intact. In the B termination these bonds are cut, creating a surface with dangling bonds and a metallic surface state[11]. In addition to these bulk terminations, a third structural model, the C termination, has been proposed by Bernasconi et al.[11]. It consists of a (1×1) reconstruction which can be thought of as two layers of Ga(III), covering the (010) surface of α-Ga. For all three terminations one would expect to observe a LEED pattern in which every odd-integer spot in the [100] direction is missing[18] because of the glide plane symmetry of bulk α-Ga which is preserved in the surface structure. The topmost layer is identical for these three structures, and therefore atomically resolved STM images, while confirming that in all likelihood one of these three structures might form, have not been able to reveal which one is actually present[6]. The STM data do suggest an additional surface relaxation, as the Ga atom in the center of the unit cell appears to be shifted by 0.2 Å towards one of the corner atoms. In the same study, the authors have reported a LEED pattern with no missing spots, consistent with the proposed relaxation, which would break the glide-line symmetry. However, a recent X-ray scattering investigation of the room temperature (RT) (1×1) phase revealed only very small lateral atomic shifts below 0.02 Å[7], not confirming the large shift of the center atom. Moreover, the RT LEED patterns reported here and in ref.[8–10] exhibits the expected missing spots. The X-ray study of α-Ga(010) has also shown that the surface structure is a B-termination of the bulk, i.e. a structure with cut Ga_2 dimers, in contrast to what was found with first-principles theory[3]. The structure of the low temperature (LT) phase has not been determined so far.

Using two similar formulations of LEED calculations we have determined the geometric structure of α-Ga(010) both for the LT and the RT phase. We find that the RT structure can be described as a "cut-dimer" surface, in agreement with the X-ray result. Below 232 K atoms from the top layer dimerize within the top layer and with atoms from the layer beneath. The bond lengths of some of these dimers are about 12% shorter than the bond lengths found in the α-Ga bulk.

II. SAMPLE PREPARATION AND LEED MEASUREMENT

An α-Ga crystal was mechanically cut from a larger bulk single crystal. The (010) surface was subsequently polished using diamond paste. The surface was then cleaned by short cycles of sputtering with 0.5-1.0 keV Ne^+ at about 273 K and annealing at the same temperature.

At 273 K a sharp (1×1) LEED pattern was observed. Every odd-integer spot in the [100] direction was missing, consistent with the glide plane symmetry of bulk α-Ga. Cooling the sample resulted in a reversible phase transition from the (1×1) to a $(2\sqrt{2}\times\sqrt{2})$R45° pattern at 232 K.

Three LEED data sets were used for the calculations reported in this study: one was measured in Berlin for the RT phase; another data set for the RT and one LT data-set were measured in Trieste. All three data-sets were measured in the normal-incidence geometry. Symmetry-equivalent beams were averaged.

For the RT data-set from Berlin, intensity versus energy curves (I-V curves)

were measured using video LEED in the rear view geometry at a sample temperature of about 265 K.

The cleanliness of the sample was monitored by Auger Electron Spectroscopy as well as by the quality of the surface state and the Ga $3d$ core levels[8]. The LEED patterns from the clean (1×1) surface as well as from the reconstructed (LT) surface exhibited very sharp spots. Five I-V curves were taken, consisting of cumulative energy range of 790 eV. The energy of the electron beam was varied in steps of 1 eV from 40-50 eV to 300 eV. The background pressure was below 10^{-10} mbar.

The second RT data-set was measured in the experimental chamber of the SuperESCA beamline of ELECTRA, Trieste at T=240 K, using a similar sample preparation and also a video LEED system. The cleanliness of the sample was monitored by X-ray photoemission spectroscopy (XPS). Five beams with a cumulative energy range of 1215 eV were taken for the RT data-set. The LT data-set consists of 9 beams with a cumulative energy range of 3064 eV and was obtained at 130 K. The background pressure was 2×10^{-10} mbar.

III. LEED I-V ANALYSIS

A. Calculation

1. *Room-temperature structure*

The RT LEED data from Berlin were analyzed using a fully-dynamical multiple-scattering code developed by Moritz[19]. The program uses the layer KKR and the "layer-doubling" method[20], combined with a search method based on analytic derivatives of the scattered amplitudes: we label this method "analytic-derivative LEED" in the following. The agreement between the calculated and measured I-V curves was quantified by the $R_{\rm P}$ reliability factor[21]. The following high-symmetry geometries were considered in the analysis: the intact-dimer surface (termination A), the cut-dimer surface (termination B) and the Ga(III) surface (termination C) [Fig.1]. The first three interlayer distances were optimized along with the position of the two Ga atoms inside the cell, using the Debye temperature for bulk Ga also for the surface layers.

In a second step the surface Debye temperature was optimized alongside another refinement of the above mentioned parameters. The optimized surface Debye temperature for the topmost layer was 180 K, the R_P-factors for the refined structures were 0.36 for the intact-dimer surface and 0.42 for the Ga(III) model. The cut-dimer model gave the best fits with an R_P of 0.25. Without an optimization of the surface Debye temperature, the R-factors for both the intact-dimer and the cut-dimer model were very close, with the intact-dimer model resulting in a slightly better fit than the cut-dimer model. An change of the Debye temperature of lower surface layers did not improve the r-factors significantly, possibly as the energy range of the beams Berlin data-set was quite limited, a lower Deybe factor however did not lead to a worse fit, either.

The second RT data-set (measured in Trieste) was subsequently analyzed with tensor LEED (TLEED) using the SATLEED package developed by Barbieri and Van Hove[23]. This is also a fully-dynamical multiple-scattering code, which differs from the analytic-derivative code by Moritz in the use of renormalized forward scattering in the search method: it is based on the tensor-LEED approximation, and reaches equivalent accuracy when iterated. The muffin-tin potential and the phase shifts were calculated using the Barbieri/Van Hove Phase Shift Package[24]. In particular, a self-consistent Dirac-Fock approach was used to compute

the self-consistent atomic orbitals for each element. The muffin-tin potential was then computed following Mattheiss' prescription and the relativistic phase shifts were evaluated by numerical integration of the Dirac equation. Three different R-factors were used here in order to quantify the agreement between theory and experiment, namely, R_P, R_1 and R_2[25]. The four models analyzed were: A termination (intact-dimer), B termination (cut-dimer), the structure resulting from our analysis of the Berlin LEED data, and the x-ray structure[7]. As the Ga(III) structure had been ruled out by a rather high R-factor in the Berlin LEED analysis, it was not included in this search. For the A and B termination the bulk values were assumed for the interlayer distances. For the first optimization only displacements perpendicular to the lattice plane were allowed, resulting in a R_P of 0.33 for the intact-dimer structure and 0.46 for the cut-dimer model. Subsequently, a detailed optimization of the surface Debye temperature (for the topmost layer only) together with the layer distances and an additional possibility for buckling in the first layer was carried out.

From Fig. 2, we can see that the R-factor depends strongly on the value of the surface Debye temperature between 100 and 320 K. The lowest R_P-factor is obtained for the cut-dimer model as 0.21 with a surface Debye temperature of 175K. In Table I, a comparison of R_P for both models at θ_D=175K and θ_D=350K is presented. The experimental and theoretical I-V curves from the Trieste data set and the TLEED calculation, respectively, are compared in Fig. 3. In this caluclation only the Debye temperature of the topmost surface layer was optimized. The value for the other layers were kept at the bulk value of 350K. In the analytic derivative LEED analysis the influence of lower Debye Temperature values for the second and third layer were additionally investigated, and found to improve the r-factor slightly.

Both the analytic-derivative and the TLEED analysis also included atomic displacements parallel to the surface as well as rumpling were considered, in the the latter only the possibility of rumpling. Although several local minima were found, they did lead to an inprovement of of the model's fit to experiment.

2. Low-temperature structure

Due to the complexity of the $(2\sqrt{2} \times \sqrt{2})$R45° LT reconstruction, it was solved exclusively with TLEED. No additional modeling was performed to take into account the long

periodicity found in the SPA-LEED study[10]. This can be justified by the relatively long domain size that makes a perturbation of the local lattice arrangement unlikely. The split ($\pm 1/2$,$\pm 1/2$)-spot was treated as one single beam; the resulting individual R-factor of this beam was, however, markedly higher than those for the remaining beams.

The $(2\sqrt{2} \times \sqrt{2})$R45° unit cell has 8 atoms per layer. Since all the symmetry is lost in this reconstruction, each atom in the unit cell can move independently in the x ([001]), y ([100]) and z ([010]) directions.

Therefore, a LEED analysis allowing 3D displacements only in the topmost layer will have at least 25 independent fit-parameters (24 structural parameters and the real part of the inner potential). It is clear that allowing more fit-parameters, for example by including the displacements in more than one layer, necessarily lowers the R-factor.The question is whether the improved fit actually implies a better structural solution. This question has been answered by the Hamilton ratio test used in bulk x-ray crystallography[26,27]. We use a modified Hamilton ratio, defined as follows: we compare a "constrained" model that has q fit-parameters and gives an R-factor R_C, with an "unconstrained" model, which has more fit-parameters p and gives a better R-factor R_U. Suppose we use $n = \Delta E_T/(4|V_{0i}|)$ experimental data points; this is a common estimate made in LEED, where the peak width $\Delta E_T/(4|V_{0i}|)$ in an I-V curve is counted as one data point. Then the Hamilton ratio can be described as depicted in the relations below[28]:

$$H = (\frac{R_C^2 - R_U^2}{p-q})(\frac{n-p}{R_U^2}).$$

Based on our experience in LEED, the Hamilton ratio H should exceed 3.0 to indicate real improvements, while values below 1.0 indicate merely a better fit due to additional parameters.

In order to investigate the influence of the number of fit-parameters on the final structure and on the R_P value we carried out the LEED analysis allowing displacements in: 1) only the first layer (24 structural parameters); 2) the first two layers (48 structural parameters, giving H=2.95 relative to structure 1); and 3) the first four layers (96 structural parameters, giving H=1.1 relative to structure 1). In each case, several different models were used as starting point during the fitting procedure. In these models various Ga-Ga dimerization in the first Ga plane were tested. As long as all top-surface Ga atoms were forced to bind to a dimer partner in the top-layer the R-factors remained (>0.60). After the atoms were

allowed to relax in x, y and z directions, minimum R-factors between 0.18 and 0.21 were obtained.

The R_P and H values for the best models for the three different numbers of fit-parameters considered for this fitting procedure are presented in Table II. As we can see, the Hamilton ratio is lower than 3 in all cases. It is, however, quite close to 3 in the case of 49 parameters. The atomic displacements of the second layer can therefore be judged to reflect the actual geometry of the reconstruction, albeit within a somewhat larger error margin than those of the first layer. The surface Debye temperature optimization resulted in a value of 160 K for the topmost Ga layer. The experimental and best-fit theoretical LEED I-V curves are shown in Fig. 4.

B. Geometry from the LEED analysis

1. Room-temperature (RT) structure

The best-fit structure for the room temperature (1×1) structure (RT) corresponds to a non-reconstructed surface, which is terminated by a layer of cut dimers. Both the analytic-derivative and the tensor LEED structures agree in the limit of their respective error margins. The structural parameters are given in Table III. The analytic-derivative LEED study finds no rumpling of the top-layer atoms, and the R_1 and R_2 yielding the best fit values of R_1=0.11; and R_2=0.22, respectively, also find no rumpling. The R_P value from the TLEED study however suggests a small rumpling of 0.092 Å. In the TLEED analysis, the surface Debye temperature was found to be 175 ± 15 K. Assuming an isotropic vibration of an harmonic oscillator[22] this value corresponds to an isotropic vibrational amplitude of 0.13 Å which amounts to 5.5 % of the Ga-Ga covalent bond length. The vibration of the top layer atoms are thus in the same range of the rumpling on the topmost layer which is suggested by the TLEED analysis's R_P. If half of the rumpling distance (0.048 Å) is added to the top layer spacing the resulting value of 1.52 Å becomes almost identical with the corresponding value of 1.53 Å from the analytic-derivative LEED study and the R_1=0.11; and R_2=0.22 r-factors. A likely interpretation of the rumpling is thus a strong (anisotropic) vibration of the top-layer atoms, rather than an actual lattice displacement. Ansotropic vibrations might be expected for surfaces which show no surface melting but are close to the melting

point.

2. Low-temperature (LT) structure

The low temperature structure is depicted in Fig. 5. The atomic coordinates are given in Table IV.

This phase exhibits the same cut-dimer termination as the room temperature structure, complicated by individual atomic displacement within the surface unit cell: the first and second layers display a partial rumpling as well as in-plane displacements. The first interlayer spacing is reduced on average by 1.5 % with respect to the bulk value, while the second and the third layer spacings were set to the bulk value.

This structure exhibits a large variation in the individual bond lengths. The variation is considerably larger than the uncertainty of about 0.1 Å̃in the bond lengths. Dimerizations of top-layer Ga atoms occur both parallel and perpendicular to the surface. The top view of the low temperature reconstruction shows the dimerizations in the plane, Table V gives a detailed overview over the next-neightbour distances of all atoms involves. Bonds which can be classified as predominately covalent dimer-bonds are listed under the notations of "ultra-short" and "short" bonds, depending whether they are equal to the dimer-bond lenght of the bulk or significantely shorter. "Medium bonds" and "long" indicate atomic distances which are in the range of metallic interactions. The 3.2 Å shell corresponds to the Ga-Ga Van der Waals radius, while the 2.95 Å value is derived by increasing the average Ga-Ga metal bond length by 10%.

The structure can be characterized in detail as follows: Two ultra-short Ga dimers form within the surface layer and similarly two Ga dimers form bonds between the first and second layers. All these bond lengths average 2.19± 0.1 Å, which is about 10% shorter than the Ga-Ga dimer bond length of 2.44 Å̃in bulk α-Ga. This arrangement, however, leaves 2 atoms per cell without any dimer bond, i.e. "dangling".

A clear difference can be seen between the populations of bond lengths for the first two layers, the ultra-short bonds occurring only for atoms bound to top-layer atoms or parallel to the top layer. The ultra-short bonds towards the second layer, which are on average contracted 9% from the bulk, are slightly longer than those inside the (010) plane, which are contracted 12%. Within the topmost layer a third dimer forms, which is 4% longer than

the bulk value.

The ultra-short dimer bonds, while being the most striking, are however not the only bonds within a covalent bonding distance for Ga. Seven to eight additional dimer bonds form between the first two layers. Assuming that a short or ultra-short next-neighbor distance indicates covalent bond formation, the degree of covalency (average number of short or ultra-short next-neighbor distances per atom) is 1.5 in the first layer, which is 50% higher than that found in the bulk. Adding the dimer bonds to the smaller number of bonds in the range of 2.62-2.84 Å, which is the range of Ga-metal bond lengths, leads to an average coordination number of 3 within a 2.95 Å shell. This is in fact the coordination one would expect for a fully covalent Ga structure. If a 3.2 Å shell is considered, the average coordination for the top layer in the LT phase is 6.0. This is still smaller than that of the semi-metallic bulk, where 7 atoms are in the range below 3.2 Å, there however occupying exclusively the range between 2.44 and 2.79 Å.

The second layer exhibits two dimers roughly inside the (010) plane; their bond length of 2.43 Å equals that of the bulk Ga-Ga dimers. This layer should dimerize with the third layer, if the simple cut-dimer surface model from the RT structure is considered. What happens to these dimer bonds? Our analysis indicates that the corresponding dimer bonds are indeed present, each atom of this layer having exactly one partner in the third layer at an average distance of 2.48 Å. These bonds are therefore slightly elongated. Atoms in the second layer display an average of 4.75 coordination partners within a 2.95 Å shell and an average number of 6.5 within a radius of 3.3 Å (80% of the Van der Waals radius of Ga). Although Ga is a trivalent element, this is an under coordination, since not all 4.75 neighbors are within the covalent distance. In the bulk α-Ga case, 7 atoms can be found within a radius of 2.9 Å. Possible factors that might contribute to this surface reconstruction are discussed in the next section.

Also in this structure, the distance in the range of 2.62-2.84 Å$\tilde{\text{i}}$s well populated: about one third of the bond lengths fall into this range. As these bond lengths are in most cases very close to those found in either liquid Ga, α-Ga or β-Ga, these distances most likely reflect quantum mechanical energy minima. Note that bond distances between the second and the third layer have however to be treated with care since the atoms in the third layer have been held at the bulk position.

An attempt to coordinate the bonds in a more symmetric fashion yielded worse R-factors.

LEED is, however, less sensitive towards distances parallel to the surface than perpendicular to the surface. Table V shows not only a detailed overview of the individual atomic distances but also gives the average values, grouped into regions, to highlight the bond length distribution most effectively. It should be noted that the separation between short and medium lengths remains an arbitrary one. We believe, however that "short" lengths have mostly covalent character, while the "medium" ones are mostly in the "metallic" range.

IV. DISCUSSION

A. Room-temperature phase

Table III gives the analytic-derivative and tensor LEED structure results as well as a comparison of our data with the X-ray analysis[7]. The two LEED analyses lead to the same structure, which is characterized by a cut-dimer termination of the topmost layer, strong atomic vibrations and a slight expansion of the topmost layer distance. Our study is in good agreement with basic outlines of the "cut-dimer" model proposed by the X-ray scattering study but differs significantly in the interlayer spacing values. As LEED is much more sensitive to the vertical interlayer spacing than X-ray scattering, we believe that our values are more reliable. The agreement for the lateral displacements with the X-ray study is very good. Neither the X-ray nor our TLEED investigation show a 0.2 Å lateral shift of the top-layer atoms as proposed by the STM study[6]; this shift is also not supported by our observed LEED diffraction pattern. Such a shift is therefore most likely absent. The uniform step height of (3.8 Å) found in that study is however consistent with our LEED result.

The B termination disrupts the dimer-bonds of the top layer. The resulting dangling bonds give rise to a surface state with a parabolic dispersion around the $\bar{C}$ point of the surface Brillouin zone, as predicted by Bernasconi et al.[11] and observed in angle-resolved photoemission[8,9]. Similar states are, however, also predicted for the other terminations. More importantly, the B-termination is the only structure which is not predicted to support any surface states in the lower lying gaps of the projected band structure and, indeed, it has not be possible to find such states in angle-resolved photoemission. In this way, the limited "structural" information which can be obtained from this technique when combined with calculations, agrees well with our result.

A remarkable result of the structural determination is the low surface Debye temperature and its unusually strong influence on the agreement between experiment and theory. In the most simple picture a low surface Debye temperature just means that the atoms vibrate strongly. Further disorder, like the presence of a small fraction of surface dimers, could also lead to a low value of the surface Debye temperature. The sharpness of the LEED diffration spots precludes however an extended presence of such disorder. Genuine surface melting can be excluded based on the STM results[6]. Thus an unisotropic component of the strong vibration seems to be most likely. This is likely as the melting point of Ga is close to room temperature.

B. Low-temperature phase

Before discussing the details of the low temperature structure as summarized in Tabs. IV and V we start with a few more general comments. In a certain sense, we may view the α-Ga structure as a layered crystal where quasi two-dimensional and metallic buckled layers are separated by covalent molecular bonds. Our room temperature results shows, in agreement with previous experiments, that the the B-termination is present and thus the crystal surface is a metallic buckled plane. In addition to this, it supports a dangling bond-type surface state which should increase its metallic character even more. At a lower temperature, however, the surface chooses to change its structure and to reduce its metallicity, as suggested by the reduced Fermi level intensity in photoemission[9]. Such a scenario is not entirely unexpected because of the fact that a two dimensional metal should be more unstable than its three dimensional counterpart.

An important characteristic feature of the LT structure is the formation of very short dimers both within the first layer as well as between the first and the second layer (see table V. This leads to a removal of dangling bonds but some of the first layer atoms also remain un-dimerized. At first glance, the removal of dangling bonds could be achieved in a much simpler way, by dimerizing the two atoms in the unit cell and keeping the periodicity (1×1). Such a type of reconstruction can, however, be excluded by the work of Bernasconi et al. who have shown that the dangling bonds point in different directions and "repel" each other[11]. The formation of a three-dimensional dimer-network apparently seems to evade this repulsion. Thus short bonds also form between the first and the second layer, i.e to a layer

in which the atoms are already dimerized.

The remaining next-neighbor bond lengths fall well in the range of atomic distances typical for α- and β-Ga[1]. The single-dimer bond in the (010) plane in the second layer has the bond length typically associated with Ga dimmers, 2.4 Å, while most of the longer next-neighbor distances in the first layer fall into the region of 2.68 Å and 2.85 Å; typical distances for β-Ga. As β-Ga is metallic these distances can be judged to facilitate an orbital overlap compatible with metallicity. The under-coordination of only 3-4.7 next neighbors of the Ga atoms in the first two layers can therefore be interpreted as a compensation for the strong covalency in this reconstruction. Our interpretation of the short distances as the evidence of a formation of covalent bonds is in agreement with both photoemission data[8,9] and the observed lower coordination numbers: an increased covalency diminishes the need for a higher, metal-like coordination. The interlayer distance between the second and the third layer is slightly enlarged and we assume that these bonds are weakened.

Having said this, we have to keep in mind the limitations of our experimental approach. The long range structure suggested by the small spot-splitting in SPA-LEED[10] suggests that the situation is much more complex than sketched here. However, the very long range of this structure and the good agreement between experimental data and LEED calculations lead us to the conclusion that we have obtained a fair description of the local structure.

In this context, as for the RT phase, the low surface Debye temperature is an interesting point which requires an explanation. There are two possible reasons. The first, like in the RT phase, is the presence of disorder caused by fact that the LT phase is not fully formed and fluctuations are present. A more likely reason, however, is that the true long range order indicated by the weak split of the (1/2 1/2/) spot in the SPA-LEED data is not included in our analysis and is interpreted as surface disorder.

The LT phase can consequently be characterized as follows: whereas in bulk α-Ga, where layers with covalent dimer bonds and layers in which metallic bonds dominate are normal to each other, at the surface this symmetry is broken and both binding mechanisms become mixed in one plane, as long as the temperature is sufficiently low. This dimerisation leads to a lateral dimerisation involving the formation of ultra-short Ga dimers within the first two layers. At higher temperatures the strong lattice vibrations prevent the formation of the necessary ultra-short dimer bonds and the dimer network is therefore disrupted.

The emerging picture of the α-Ga surface phase transitions between 200K and 350K is

therefore dominated by a disruption of covalent bonds with increasing temperature. Metal to covalent phase transitions have been found for bulk non-transition metals, in particular Sn[30], which transforms into covalent, non-metallic modifications at lower temperatures. Si and C become likewise metallic in the liquid (molten) state. The surface transition described for α-Ga in this paper is however intriguing as it concerns a trivalent metal with a much reduced electron density and the effect is limited to the surface region.

V. CONCLUSIONS

The geometric structure of the α-Ga(010)-(1×1) room temperature structure has been determined with both analytic-derivative and TLEED. The structure was confirmed to be the B-termination, i.e. the cut-dimer model. The first interlayer distance is 1.53 Å: an expansion of 2% from the bulk value. The low temperature $(2\sqrt{2} \times \sqrt{2})$R45° phase has been determined using TLEED. Atoms from the outermost layer dimerize within that layer and with atoms in the layer beneath it. The bond lengths of these dimers are reduced by more than 10% compared to the bond lengths found in the α-Ga bulk and are the shortest Ga-Ga bonds reported so far, setting a new reference for covalent Ga bonds. The phase transition can be achieved by a mere distortion of the RT structure. No major mass transport is required.

VI. ACKNOWLEDGMENTS

This work was supported in part by the Director, Office of Science, Office of Basic Energy Sciences, Division of Materials Sciences and Engineering, of the U.S. Department of Energy under Contract No. DE-AC03-76SF00098, by the Danish National Research Council and by the Carlsberg Foundation. EAS would like to thank CNPq and FAPESP, Brazilian research agencies, for financial support. We would further like to thank M. Bernasconi for valuable discussions.

---

* philip@phys.au.dk; http://www.phys.au.dk/~philip/

* Former address: Fritz-Haber-Institut der Max-Planck- Gesellschaft, Faradayweg 4-6, D-14195 Berlin, Germany, Electronic mail address more@ims.ac.jp

** Present address: Depto de Fisica - ICEX - UFMG, CP 702, Belo Horizonte, MG, 30161-970, Brazil.

[1] Gmelin, Handbook of Inorganic and Organometallic Chemistry, Vol. 36.

[2] R.W.G. Wyckhoff, Crystal Structures, John Wiley, New York and London, (1963).

[3] X.G Gong, G.L. Chiarotti and M. Parrinello and E. Tosatti, Phys. Rev. B, **43**, 14277, 1991; Bernasconi, M. and Chiarotti, G. L. and Tosatti, E., Physical Review B, **52**, 9988, 1995.

[4] Note that there are different conventions in use for the crystallographic directions in α-Ga. We and ref. 7–9 follow the crystallographic convention ($Cmca$ symmetry) while ref. 3,6,11 follow the historic (pseudotetragonal) convention. In the latter case the b and $\bar{c}$ axes are reversed and the structure have the nonstandard $Mbab$ symmetry. Our (010) surface corresponds to the (001) surface in this case.

[5] R. Trittibach, Ch. Grutter and J.H. Bilgram, Phys. Rev. B **50**, 2529 (1994).

[6] O. Zueger and U. Durig, Phys. Rev. B **46** 7319 (1992); O. Zueger and U. Duerig, Ultramicroscopy **42-44**, 520 (1992).

[7] D.A. Walko, I. K. Robinson, Ch. Grütter and J.H. Bilgram, Phys. Rev. Lett. **81**, 626 (1998).

[8] P. Hofmann, Y.Q. Cai, Chr. Grütter and J.H. Bilgram, Phys. Rev. Lett. **81** 1670 (1998).

[9] Ch. Søndergaard, Chr. Schultz, A. Angergaard, H. Li, S.V. Hofmann, Z. Li, Ph. Hofmann, Chr. Grütter and J.H. Bilgram, (to be published).

[10] S. Lizzit, A. Baraldi, Ph. Hofmann, Chr. Grütter and J.H. Bilgram, (to be published).

[11] M. Bernasconi, G.L. Chiarotti and E. Tosatti, Phys. Rev. Lett, **70**, 3295 (1993); M. Bernasconi, G.L. Chiarotti and E. Tosatti, Phys. Rev.B **52**, 9999 (1995).

[12] Plummer, E.W. and Hannon, J.B., Prog. Surf. Sci., **46**, 149, (1994).

[13] Ph. Hofmann, R. Stumpf, V. M. Silkin, E. V. Chulkov and E. W. Plummer , Surf. Sci., **355**, L278, (1996).

[14] M. Hengsberger, P. Segovia, M. Garnier, D. Purdie and Y. Baer, The European Physical Journal B **17**, 603 (2000).

[15] S. Agergaard, Ch. Søndergaard, H. Li, M. B. Nielsen, S. V. Hoffmann, Z. Li and Ph. Hofmann, New Journal of Physics **3**, 15.1 (2001).

[16] C.R. Ast and H. Höchst, Phys. Rev. Lett., **87**, 177602, (2001).

[17] E. Tosatti in *Electronic Surface and Interface States on Metallic Systems* (eds. E. Bertel and M. Donath) World Scientific, Singapore (1995).

[18] B. W. Holland and D. P. Woodruff, Surf. Sci. **36**,488 (1973).

[19] W. Moritz, J. Phys. C **17**, 353 (1988).

[20] J.B. Pendry, *Low Energy Electron Diffraction* (Academic Press, London, 1971).

[21] J.B. Pendry, J. Phys. C **13**, 937 (1980).

[22] S. Schwegmann, H. Over, Surf. Sci. **360**, 271 (1996).

[23] A. Barbieri and M.A. Van Hove, (http://electron.lbl.gov/leedpack/).

[24] Barbieri/Van Hove Phase Shift Package: http://electron.lbl.gov/leedpack/leeadpack.html.

[25] M.A. Van Hove, W.H. Weinberg and C.-M. Chan, *Low-Energy Electron Diffraction: Experiment, Theory and Structural Determination*, Springer Series in Surface Sciences, Vol. 6, Springer-Verlag (Berlin, Heidelberg, New York, 1986).

[26] W. C. Hamilton, Acta Crystall. **18**, 502 (1965).

[27] E. Prince, *Mathematical Techniques in Crystallography and Materials Science* (Springer-Verlag, New York, 1982).

[28] E.A. Soares, M.A. Van Hove, C.F. Walters and K.F. McCarty, Phys. Rev. B, **65** 195405 (2002).

[29] O. Tomagnini, F. Ercolessi, S. Iarlori, F.D. DiTolla and E. Tosatti, Phys. Rev. Lett. **76** 1118 (1996).

[30] P.Pavone, S. Baroni, S. deGironcoli, Phys. Rev. B **57** 10421 (1998).

FIG. 1: α-Ga elementary cell for the A (intact dimer) termination, B (cut dimer) termination and the C (Ga(III)) termination, as discussed in the text. The lines joining two atoms symbolize the covalent Ga dimers

FIG. 2: R-factor values R_P, R_1 and R_2 as a function of the Debye temperature in the LEED calculation

FIG. 4: bf LEED I-V curves for the LT surface structure. Dashed lines: experimental curves. Solid lines: theoretical curves for the best model obtained for the α-Ga(010)-$(2\sqrt{2}\times\sqrt{2})$R45° structure, with best-fit atomic coordinates in the first two layers.

FIG. 5: Top view of the LT structure model. The atoms are labeled according to Table IV. Topmost atoms are black, the atoms in the layer below dark grey, atoms in the 3rd layer light grey, atoms in the 4th layer white.

TABLE I: R-factors of the different terminations from TLEED as a function of the Debye temperature

Debye temperature [K]	R-factor R_P	
	Termination B (cut-dimer)	Termination A (intact-dimer)
175	0.21	0.36
350	0.34	0.30

FIG. 3: LEED I-V curves for the RT (room temperature) surface structure. Dashed lines: experimental curves. Solid lines: theoretical curves for the best model obtained for the α-Ga(010)-(1×1) surface, with best-fit atomic coordinates in the first two layers.

TABLE II: R_P and H values for the best models for three different numbers of fit parameters to evaluate the significance of the number of fitting parameters. H is calculated with respect to the first model.

number of layers	number of fit-parameters	R_P	H
1	25	0.30	
2	49	0.21	2.98
4	97	0.18	1.13

TABLE III: R-factors and geometrical parameters of the different models for the high temperature (1×1) α-Ga phase: d_{12} through d_{45} are the topmost 4 interlayer spacings; the buckling refers to the topmost layer only; Δ x-y represents displacements parallel to the surface in the [001] and [100] directions. The values in brackets result if a buckling is permitted and arises only for the R_P optimization with the TLEED program, but not if the R-factor is changed to R_2 or R_1. The bulk interlayer spacings are 1.47 Åand 2.36 Å, alternating.

	Geometrical parameters in [Å]					
	Termination B (cut-dimer)			Termination A (intact-dimer)		Termination C (Ga(III))
	Tensor LEED	analytic-derivative LEED	X-ray study[7]	Tensor LEED	analytic-derivative LEED	
d_{12}	1.52 ±0.03 (1.49)	1.53 ±0.03	1.337	–	–	–
d_{23}	2.38 ±0.03	2.36 ±0.03	2.597	2.35	2.35	1.66
d_{34}	1.43 ±0.05	1.43 ±0.05	1.459	1.47	1.48	1.52
d_{45}	2.38 ±0.05	2.36	2.3759	2.35	2.38	2.29
buckling	none (0.09)	none	none	none	none	
R-factor (R_P)	0.21	0.25	LEED-R_P =0.82	0.30	0.36	0.42
Δ x-y	none	none	smaller than 0.05 Å	none	none	0.332, 0.03
Debye T [K]	175	180	-	175	175	175

TABLE IV: Geometrical parameters of the LT structure; atomic displacements are given as $\Delta = (x,y,z)_{reconstruction}$-$(x,y,z)_{bulk}$ in [Å]; layer spacings $d_{i,j}$ are given in [Å]. The x, y and z directions are parallel to the [001], [100], and [010] crystallographic directions, respectively.

The error margins for the topmost layer atoms 1-8 are 0.2 Å in the x and y directions and 0.05 Å in the z-direction. The error margins for the second layer atoms 9-16 are 0.2 Å in the x and y directions and 0.08 Å in the z-direction.

atom	Positions (bulk)			displacements		
	x	y	z	Δx	Δy	Δz
1	0.000	0.000	0.000	-0.46	0.27	-0.05
2	4.526	0.000	0.000	-0.44	0.06	0.00
3	6.065	2.256	0.000	0.04	0.67	-0.27
4	6.065	-2.256	0.000	-0.28	-0.22	0.11
5	10.590	-2.260	0.000	0.22	0.45	-0.04
6	9.052	-4.519	0.000	0.14	-0.37	-0.04
7	10.590	-6.779	0.000	-0.41	-0.65	-0.03
8	4.526	-4.519	0.000	0.21	-0.25	-0.01
9	2.233	0.000	1.472	0.11	0.27	-0.20
10	6.789	0.000	1.472	-0.00	-0.04	0.03
11	8.328	2.260	1.472	-0.05	0.13	-0.03
12	8.328	-2.260	1.472	0.27	0.38	0.07
13	12.860	-2.260	1.472	0.05	-0.14	-0.11
14	11.315	-4.519	1.472	-0.01	-0.06	-0.03
15	12.860	-6.779	1.472	-0.27	0.21	0.09
16	6.789	-4.519	1.472	-0.27	0.36	-0.03

$d_{i,j}$	Ga bulk	Ga LT reconstruction
d_{12}	1.49	1.472
d_{23}	2.38	2.38
d_{34}	1.49	set as bulk
d_{45}	2.38	set as bulk

TABLE V: Near-neighbor distances (bond lengths) found for the the atoms A_i in the first two layers of the LT reconstruction. Listed are also the total number of bonds per atom in the metallic and covalent bonding range ($< 2.95\mathring{A}$) shell and the Van der Waals bonding range ($< 3.3\mathring{A}$). The labels "same", "2nd", "3rd" and "others" refer to bonding atoms in the same or different layers.

first layer atom distances (Å)												
	ultra-short		short		medium		long		very long		total	total
i	same	2nd	same	2nd	same	to 2nd	same	2nd	same	2nd	< 2.95	< 3.3
1	2.08	–	–	2.45, 2.39	–	–	–	2.79	3.19	3.22	4	6
2	–	2.27	–	–	–	2.69	–	2.84	3.05, 3.06	3.06	3	6
3	–	–	–	–	–	–	–	2.84	3.19, 3.04,	3.14, 3.01, 3.03	1	7
4	–	2.22	2.54	2.51	–	–	–	–	3.06,	2.95, 3.13,	3	6
5	2.21	–	–	–	–	2.57, 2.59, 2.61	–	–	3.19	3.37	4	6
6	–	–	–	–	–	2.64	–	2.89	3.19, 3.03,	3.07, 3.03, (3.4)	2	5
7	2.08	–	–	2.36, 2.37	–	–	–	–	3.03, (3.33)	2.99, (3.43)	3	6
8	2.21	–	2.54	2.35, 2.45	–	–	–	–	–	2.96, 3.31,	4	6

second layer atom distances (Å)																
	same	other		same	other		same	other		same	other		same	other		total	total
i	–	1st	3rd	–	1st	3rd	–	1st	3rd	–	1st	3rd	–	1st	3rd	< 2.95	< 3.3
9	-	2.27	–	2.51,	2.37	2.49	–	–	–	2.77	–	–	(3.56)	3.22, 3.14, (3.36)	–	5	6
10	–	–	–	–	–	2.49	2.58	–	–	2.85	–	–	–	2.96, 2.95, 3.01, 3.06	–	3	7
11	–	–	–	–	2.51	2.41	–	2.59, 2.69	–	2.77, 2.85,	2.84	–	–	3.31	–	7	7
12	–	–	–	–	2.35	2.54	2.58	–	–	–	–	–	3.08, 3.32,	3.07, 3.13	–	3	7
13	–	–	–	–	2.37, 2.38	2.49	–	2.61	–	2.71	2.89	–	3.32	–	–	6	7
14	–	–	–	2.41	2.45	2.38	–	2.64	–	2.71	–	–	–	3.22	–	5	6
15	–	–	–	2.51, 2.41	–	2.57	–	–	–	–	2.84, 2.79	–	–	2.99, 3.03,	–	5	6
16	–	2.22	–	–	2.45	2.54	–	2.57	–	–	–	–	3.08, 3.32	3.03	–	4	7

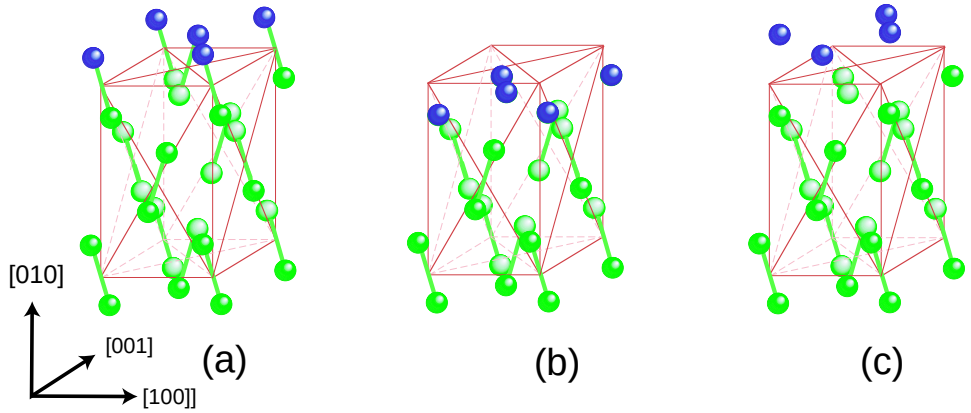

Fig. 1

Figure 1 BX8224 20OCT02

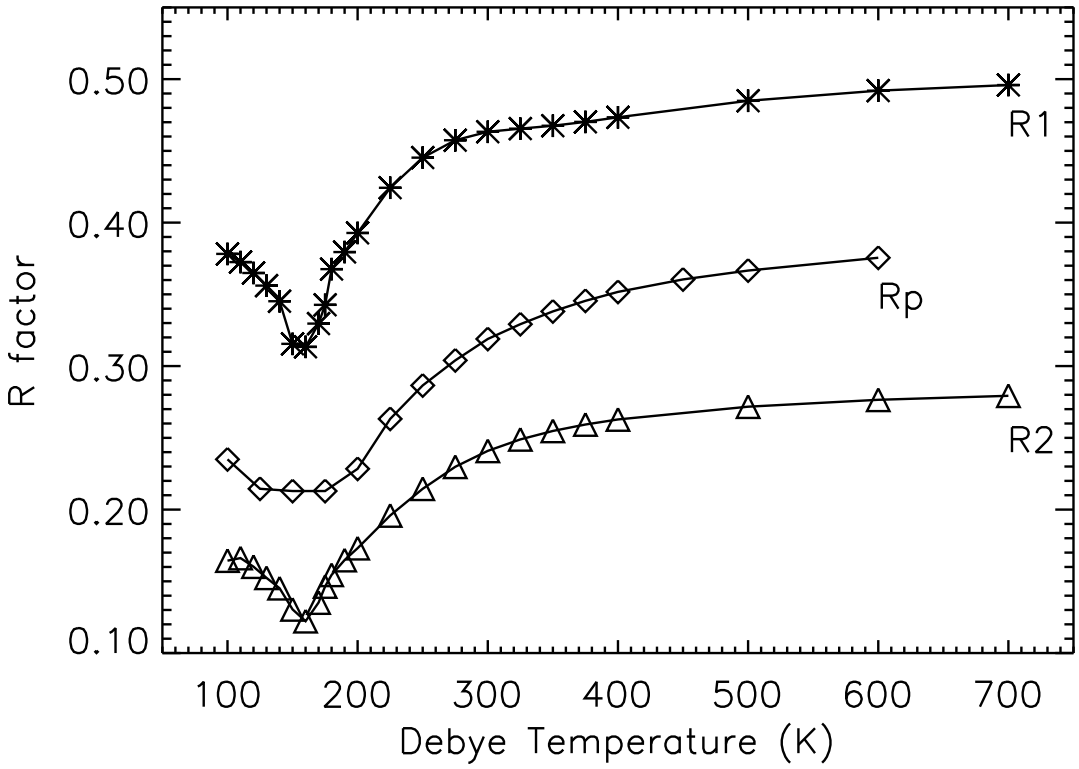

Figure 2 BX8224 20OCT02

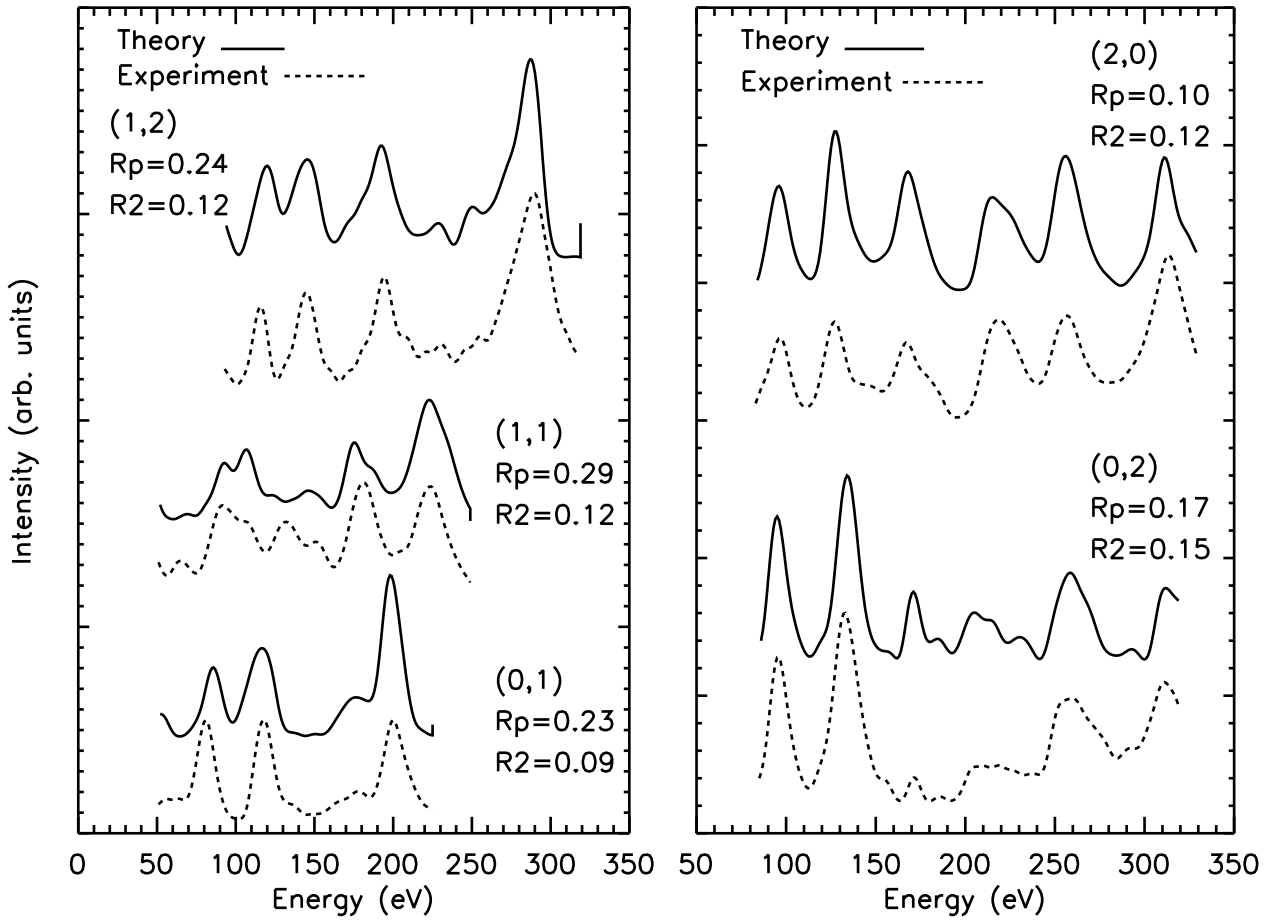

Figure 3 BX8224 20OCT02

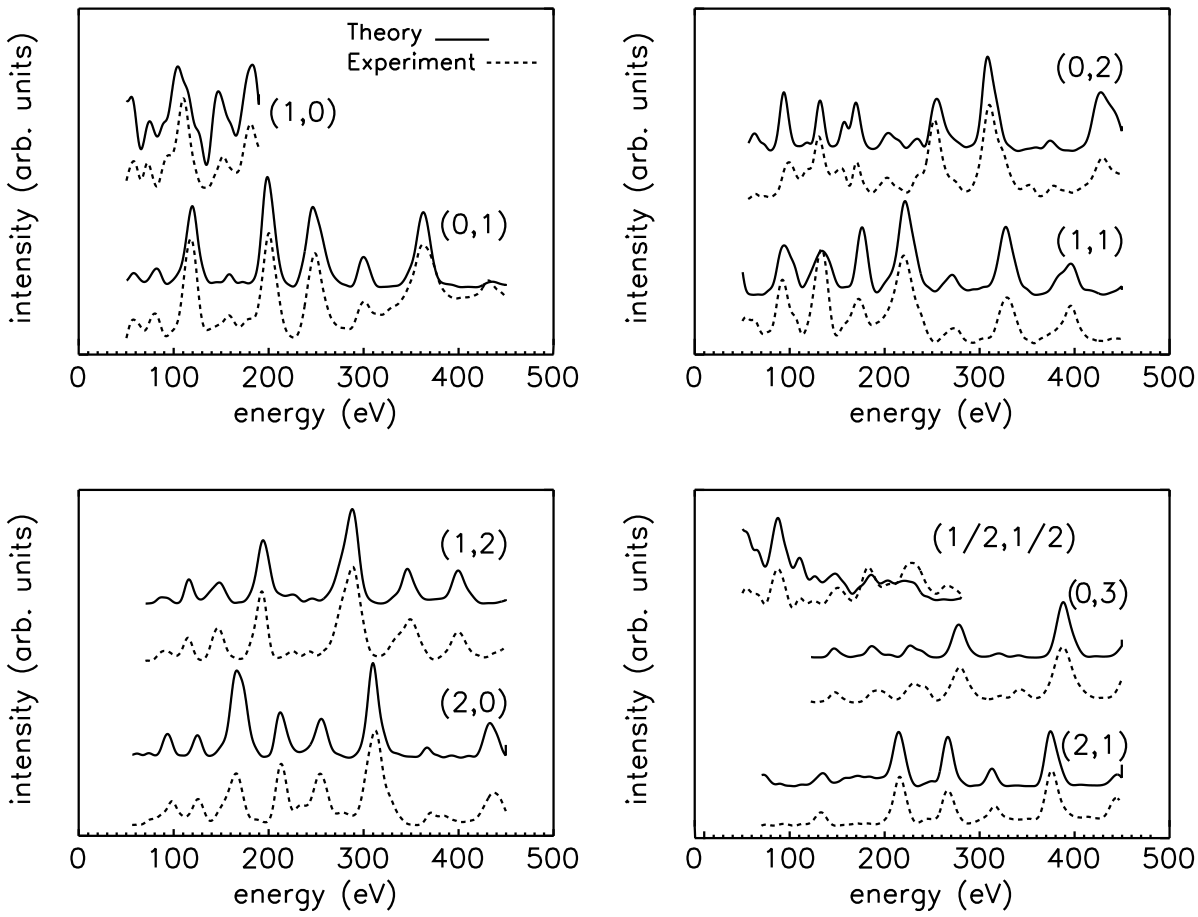

Figure 4 BX8224 20OCT02

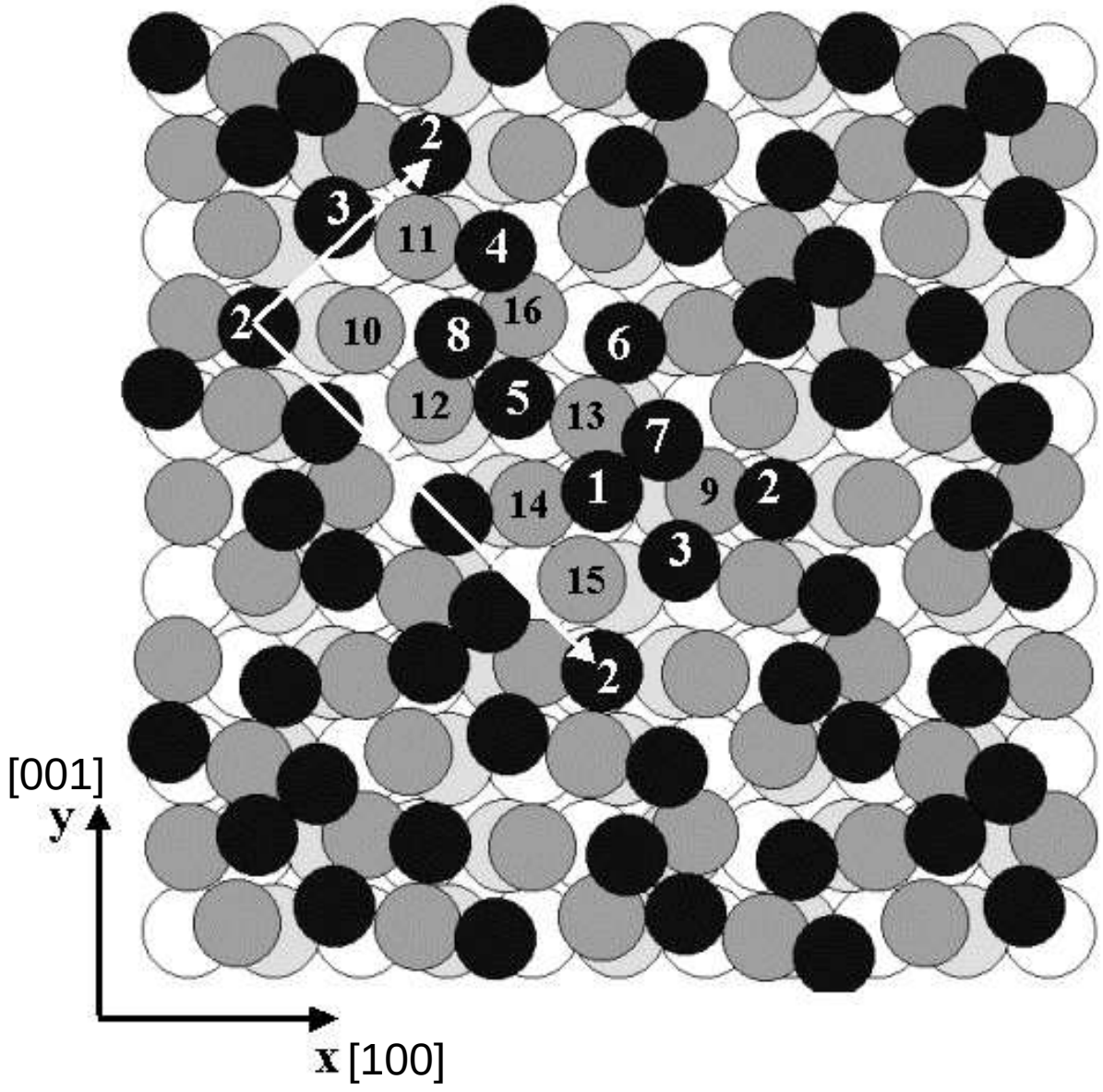

Figure 5 BX8224 20OCT02